



# Hypercrosslinked porous polymer as catalyst for efficient biodiesel production

S. Señorans<sup>a</sup>, E. Rangel-Rangel<sup>b</sup>, E.M. Maya<sup>b</sup>, L. Díaz<sup>a,\*</sup>

<sup>a</sup> Departamento de Ingeniería Química, Universidad de La Laguna, Avda. Astrofísico Fco. Sánchez s/n, La Laguna, Tenerife, Islas Canarias 38200, Spain

<sup>b</sup> Departamento Fronteras en Química de Materiales, Instituto de Ciencia de Materiales de Madrid (ICMM-CSIC), Sor Juana Inés de la Cruz, 3, Cantoblanco, Madrid 28049, Spain

## ARTICLE INFO

### Keywords:

Biodiesel  
Free fatty acid  
Heterogeneous catalyst  
Hypercrosslinked porous polymers  
Basic porous solid

## ABSTRACT

While porous organic polymers (POPs) are known for their unique properties, their application in basic biodiesel catalysis is innovative. This study introduces a novel catalyst, hypercrosslinked polymer (HCP-SB-K), synthesized through mechanochemical polymerization of styrene and benzaldehyde with a cross-linking agent and FeCl<sub>3</sub>, followed by calcination of the previous polymer impregnated with KNO<sub>3</sub>. The synthesis costs 3.328 euros per gram of catalyst, covering energy and reagent expenses. The catalyst's basic character is explored, demonstrating efficient transesterification with diverse feedstocks. Under optimal conditions, the HCP-SB-K catalyst exhibits exceptional catalytic activity, yielding 99.9% FAME (Fatty Acid Methyl Esters) at 60 °C, 2 h and 3% w/w catalyst. Investigation of free fatty acid (FFA) content highlights the catalyst's effectiveness with oils varying FFA levels: oils with acid value of 0.44 mg<sub>KOH</sub> g<sub>oil</sub><sup>-1</sup> reached 92.1% FAME at 60 °C, 1 h and 3% w/w catalyst; oils with an acid value of 1.11 mg<sub>KOH</sub> g<sub>oil</sub><sup>-1</sup>, reached 75.9% FAME, under the same conditions. Catalyst leaching evaluation indicates no discharge of basic sites. The regenerated catalyst (impregnation with KNO<sub>3</sub> and calcination, after the first use) exhibits a 98.2% FAME like the fresh catalyst. This suggests that HCP-SB-K can be regenerated without noticeable deactivation, emphasizing its industrial potential.

## 1. Introduction

In recent years, biodiesel has gained increasing attention as a viable alternative to fossil fuels. Biodiesel, primarily composed of Fatty Acid Methyl Esters, is derived from vegetable oils and animal fats. Several methods are available for biodiesel production, including micro-emulsification, blending, thermal cracking, and transesterification. Transesterification is the most widely adopted method due to its simplicity and the acceptable fuel characteristics it produces [1]. The transesterification reaction involves the interaction of triglyceride molecules with low molecular weight alcohols (methanol) to produce esters (FAME) and glycerol. The overall transesterification reaction proceeds in a molar ratio of alcohol to triglyceride of 3 to 1, in practice, an additional amount of alcohol is often added to drive the reaction towards the formation of methyl esters. However, while transesterification offers numerous advantages, including high conversion rates and straightforward operation, it is not without its challenges.

One significant challenge lies in the use of homogeneous catalysts, such as KOH or NaOH, which are commonly employed at the industrial

scale to enhance reaction kinetics. Despite their efficacy, these catalysts are susceptible to the presence of water and free fatty acids in the reaction medium, leading to undesirable side reactions such as hydrolysis and saponification. Consequently, the formation of soaps consumes catalyst and reduces the yield of biodiesel, complicating glycerol separation and necessitating post-transesterification purification steps [2]. To overcome these drawbacks, researchers are exploring various solid-based catalysts, focusing on modifying its basicity, surface area, and porosity [3]. Heterogeneous catalysts can be easily separated from reaction products without the need for water washing, thereby avoiding undesired saponification reactions and potentially reducing production costs. Among numerous basic heterogeneous catalysts, metal oxides, mixed metal oxides, and alkali hybrids catalysts have been the most studied for biodiesel production [4]. Calcium oxide (CaO) stands out among heterogeneous catalysts, derived from sources like eggshells, snail shells, biont shells, and many more. It exhibits high catalytic activity for transesterification, is cost-effective, and environmentally friendly. However, CaO catalysts have limitations, including deactivation due to leaching and sensitivity to free fatty acids (FFA),

\* Corresponding author.

E-mail address: [laudiaz@ull.edu.es](mailto:laudiaz@ull.edu.es) (L. Díaz).

necessitating pretreatment steps and increasing production costs [5]. To address these challenges, researchers are intensifying efforts to find highly active heterogeneous catalysts, including those derived from agricultural waste [6] and metal-organic frameworks (MOFs) [7,8]. These catalysts show promise in offering enhanced catalytic activity and selectivity for biodiesel production. In this context, porous organic polymers (POPs) are very promising materials to be used as heterogeneous catalysts for biodiesel production due to their unique properties such as huge surface area, tunable porosity, high hydrothermal and mechanical stability [9]. Moreover, they are excellent platforms for incorporating functionalities, such as acid or basic active centers. POPs cover many different types of networks among which the most studied have been conjugated microporous polymers (CMPs), covalent organic frameworks (COFs), covalent triazine frameworks (CTFs), polymers of intrinsic microporosity (PIMs) and hypercrosslinked polymers (HCPs). Among all of these, HCPs stand out for their easy and accessible synthesis which consists of a Friedel-Craft reaction between aromatic monomers [10–12]. Thus, some hypercrosslinked porous networks followed by sulfonation have been reported as efficient and stable acid catalysts for biodiesel production [13,14].

Furthermore, as biodiesel gains prominence as a fossil fuel alternative, cost reduction becomes a critical priority, research has expanded to explore a diverse range of feedstock sources, including single oil feedstocks such as edible vegetable oils, non-edible vegetable oils, animal fats, waste cooking oil, and algal oil [15], as well as, blended feedstock to overcome the constraints of single oil feedstock-based biodiesel production [16,17]. However, the quality and efficiency of the transesterification process are influenced by the feedstock's quality, such as the fatty acid composition and physicochemical properties.

Therefore, this study addresses the aforementioned challenges by introducing a novel hypercrosslinked polymeric catalyst (HCP-SB-K) for biodiesel production, synthesized through a mechanical polymerization followed by an impregnation and partial calcination process. While previous research has focused primarily on acidic HCP-based catalysts for biodiesel production, this work pioneers the exploration of a polymeric network with a basic character. From the perspective of catalyst preparation, a more sustainable synthesis procedure was employed. This involved utilizing mechanochemical synthesis to obtain the initial polymeric support in the absence of solvent within just 1 h. Subsequently, the introduction of basic active centers was achieved through impregnation and partial calcination. From the perspective of biodiesel production, this exploration aims to enable the utilization of several feedstocks (oils) as raw materials, evaluating the effect of the free fatty acid content on the performance of the transesterification reaction, as well as the reaction time and the reuse of the catalyst. Therefore, this work represents the first step towards establishing a basic hypercrosslinked polymeric catalyst as a versatile and efficient tool for biodiesel production from diverse feedstock sources.

## 2. Experimental

### 2.1. Chemicals and materials

Styrene (99,9%) and methanol (MeOH) (99,8%) were supplied by Sigma-Aldrich (Germany). Benzaldehyde (98%) and dimethoxymethane (98%) were provided by Alfa Aesar (USA). Iron trichloride (98%) was supplied by Fisher Chemical (USA).  $\text{KNO}_3$  (99%) was supplied by Panreac (Spain). Moreover, diethyl ether, contains 1 ppm BHT as inhibitor, anhydrous, ( $\geq 99,7\%$ ) was supplied by Sigma-Aldrich (USA), ethanol (96% v/v) by Scharlau (Spain), phenolphthalein solution 1% in ethanol by Merck (Germany) and potassium hydroxide solution 0.1 N in ethanol by Honeywell Fluka™ (Germany). Various oil types were employed as reactants for transesterification reaction. The tested feedstocks comprised a commercially available edible-grade oil obtained from the market (sunflower oil), *Jatropha curcas* oil extracted from its seeds, and three waste oils from frying foods: waste cooking I sourced from a

cafeteria at the University of La Laguna, as well as waste cooking II and III sourced from restaurants. *Jatropha curcas* oil was extracted from its seeds using n-hexane ( $\geq 97,0\%$ , Sigma-Aldrich, Israel) as a solvent, employing a soxhlet extractor. The resulting oil was esterified to reduce its free fatty acid content. The detailed processes for extraction and esterification can be found in a previous work [18]. Furthermore, the esterified *Jatropha curcas* oil was also evaluated as a feedstock for biodiesel production.

### 2.2. Catalyst synthesis

The mechanochemical synthesis was performed on a planetary ball mill Retsch PM100 model (Germany) with Fritsch 50 mL steel-cased zirconia grinding bowls, 2 cm zirconia grinding balls, and Viton seal O-rings.

The synthesis of the basic hypercrosslinked porous polymer catalysts (HCP-SB-K) was carried out in two steps:

#### 2.2.1. Synthesis of HCP-SB

Styrene (0.5 mL, 4.17 mmol), benzaldehyde (0.42 mL, 4.17 mmol) and iron (III) chloride (6.6 g, 41 mmol) were added to a zirconia vessel with three zirconia balls (mechanochemical synthesis). Dimethoxymethane (3.6 mL, 41 mmol) was added and the mixture was ball-milled at 600 rpm for 1 h. After milling, MeOH was added to the vessel, and the product was filtered out. The solid was washed with  $\text{NH}_4\text{OH}$ , diluted HCl, and water and finally purified by Soxhlet extraction with MeOH for 1 day. The solid was dried under vacuum at 100 °C for 24 h to obtain HCP-SB in quantitative yield (0.9 g) as garnet powder.

#### 2.2.2. Synthesis of HCP-SB-K

$\text{KNO}_3$  was introduced into HCP-SB by a modified impregnation method. Typically, a 50 mL flask was charged with 750 mg of  $\text{KNO}_3$  and 20 mL of deionized water; then, 0,8 g of HCP-SB was introduced in the flask and stirred for 24 h at room temperature. Finally, the deionized water was removed by a rotary evaporator, and the solid was dried at 100 °C in a vacuum oven overnight. This solid was then calcined at 350 °C in a  $\text{N}_2$  flow for 2 h to decompose  $\text{KNO}_3$  into basic sites obtaining 1.1 g of black power denoted as HCP-SB-K.

### 2.3. Catalyst characterization

ATR-FTIR spectra were recorded on a PerkinElmer Spectrum Two spectrometer with a Fourier equipped with a diamond internal element (L160000A USA).  $^{13}\text{C}$  solid-state MAS-NMR measurements were recorded with a Bruker AV400 WB spectrometer (L2.5 170-31P/19F-1H, Germany). X-ray Photoelectron Spectroscopy (XPS) data were recorded in a SPECS GmbH system equipped with a hemispherical energy analyzer PHOIBOS 150 9MCD (Germany). A non-monochromatic Mg X-ray source was used with a power of 200 W and voltage of 12 kV. Samples were introduced in the pre-chamber at room temperature and degassed for several hours before being transferred to the analysis chamber. Pass energies of 50 and 20 eV were used for acquiring both survey and high-resolution spectra, respectively. Thermogravimetric and differential thermal analyses (TGA-DTA) were recorded on a TA Instruments Model TA-Q500 analyzer (USA). The samples were heated from 40 to 800 °C under  $\text{N}_2$  atmosphere with a heating rate 10 °C/min. Specific surface areas and porosity analysis were determined by  $\text{N}_2$  adsorption/desorption isotherms on a Micromeritics, ASAP 2020 MICROPOROUS DRY Analyzer (USA) (P/Po 0.01–1.0) using the BET theory, BJH and DFT methods. Before each measurement, the sample was degassed at 110 °C for 12 h. The morphology was also analyzed by scanning electron microscopy (SEM) obtaining micrographs with a Hitachi SU-8000 microscope (Japan) operating at 0.5 kV. Chemisorption analysis was carried out through the temperature-programmed desorption profiles of  $\text{CO}_2$  ( $\text{CO}_2$ -TPD) using apparatus equipped with a mass detector (AutoChem II 2920 V4.01 A model from Micromeritics

Instrument Corp., USA). Before the CO<sub>2</sub>-TPD experiment, sample (0.1005 g) was treated in situ in a helium flow heating the sample at 110 °C at 10 °C/min for 15 min. The sample was then exposed to CO<sub>2</sub> to an initial temperature of 80 °C and with a ramp of 10 °C/min for 60 min and then heated to 320 °C at 10 °C/min under a Helium flow while it was monitoring the desorption of CO<sub>2</sub>.

#### 2.4. Oil characterization

The viscosity and density of the oils were measured using a Visco Star Plus L rotational viscometer (Fungilab S.A., V50003 code, Spain) and a Densito 30PX portable densimeter (Mettler Toledo, LWE01101, Japan), respectively. Moreover, to assess the level of free fatty acids in the oil samples, the acid value (AV) of the oil was determined through a titration method according to the UNE-EN 14104 [19]. Additional details about the method are documented in the Supplementary Information. For qualitative determination of triglycerides present in the oils a FTIR spectrophotometer (Agilent Cary 630 FTIR, G8043AA model number, USA) was used, which is equipped with attenuated total reflectance (ATR). The ATR unit, with a ZnSe crystal, was employed in the wavelength region of 1000–2000 cm<sup>-1</sup>. The unit was controlled using the Cary 630 MicroLab software, and data processing was performed using the Resolutions Pro program. Additional details about the method are described in the Supplementary Information.

#### 2.5. Transesterification reaction

The transesterification reaction was carried out in a 50 mL three-neck round bottom flask equipped with a condenser and a heater with a magnetic stirrer (Fig. 1). The photo of the reaction system used for biodiesel production is shown in the Supporting Information (Fig. S1). Initially, 30 mg of HCP-SB-K catalyst was added to the flask followed by the addition of 1 g of oil and 7.29 g of methanol. The reaction temperature was adjusted to 60 °C and the reaction time was varied between 0.5 and 2 h. During the transesterification reaction, the stirring speed was maintained at 500 rpm. This stirring speed has been widely recognized in the literature as optimal for transesterification reactions, particularly when heterogeneous catalysts are used for biodiesel production [20]. Once the reaction was complete, the catalyst was separated by vacuum filtration from the resulting mixture. The reaction products were transferred to a test tube and left in an oven overnight to evaporate the excess methanol. This resulted in the formation of two distinct phases: the upper phase rich in FAME and the lower phase rich

in glycerol. Each transesterification reaction was conducted in triplicate, and subsequently, the FAME content was measured in triplicate according to the procedure outlined in Section 2.8, with the mean value subsequently calculated. Additionally, the standard deviation was determined to assess the variability of the results.

To ensure the need for the basic centers in this catalyst, a control experiment was carried out using the starting support (HCP-SB) as a catalyst. Additionally, the same reaction was carried out using iron (III) chloride (6 mg) for a duration of 1 h, following the procedure described previously. The presence of 20% residual iron in the basic catalyst was observed (2 mg of Fe in 10 mg of catalyst). For this reason, a control experiment was carried out using an excess of FeCl<sub>3</sub> as a catalyst to evaluate the catalytic activity of this solid and its impact on the reaction yield.

#### 2.6. Catalyst leaching evaluation

The contribution of homogenous catalysis due to catalyst leaching was assessed. For this test, a transesterification reaction was carried out using sunflower oil and a fresh catalyst, employing typical reaction conditions (1 g of oil, 7.26 mL of methanol, 30 mg of catalyst and, a temperature of 60 °C). After 0.5 h, the catalyst (HCP-SB-K) was separated from the mixture by filtration, and the FAME content was determined. Subsequently, the reaction mixture, devoid of the catalyst, was continuously stirred for an additional 2 h, following which the FAME content was determined once more.

#### 2.7. Recycling and regeneration evaluation

To investigate the potential reusability of the catalyst, 60 mg of HCP-SB-K catalyst was employed, and the quantities of oil and methanol were recalculated for each cycle. This adjustment aimed to maintain the same conditions in all cycles. After each reaction, the HCP-SB-K catalyst was recovered, washed with ethanol, and dried at 70 °C overnight. The regeneration process was also developed. Subsequent to undergoing the washing and drying process, the used catalyst was subjected to the impregnation and calcination process, as described in Section "Synthesis of HCP-SB-K". Its catalytic activity in the transesterification reaction was then studied. The potassium content of the catalysts was determined by atomic absorption spectrometer (Varian 220FS Spectra AA, USA). Prior to measurement, the catalyst powder was digested using a microwave digestion method (Ethos Touch Control, Milestone, USA).

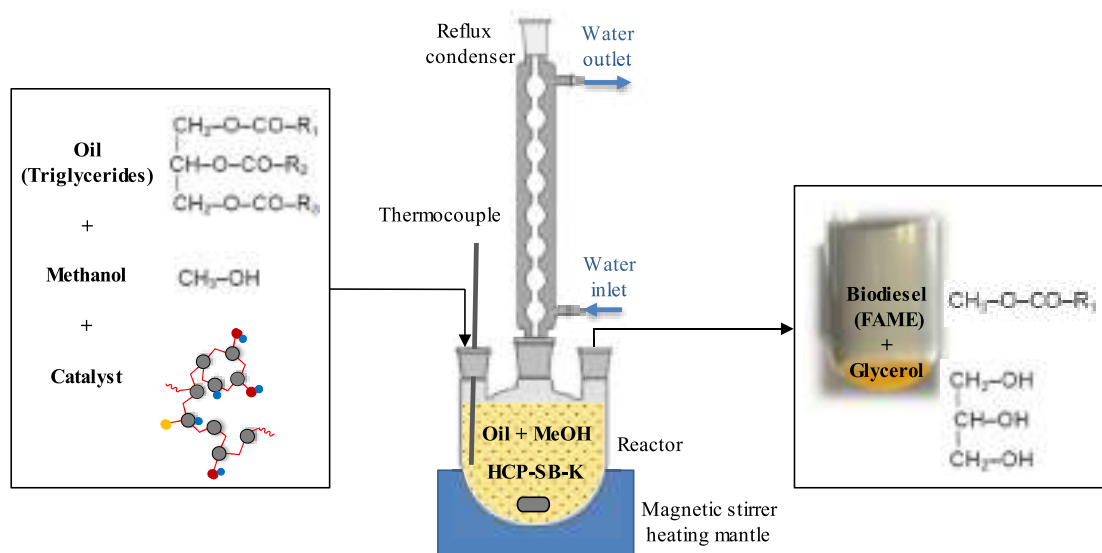


Fig. 1. Scheme of the reaction system for the biodiesel production.

## 2.8. Products analysis

The biofuel obtained from the transesterification reaction, specifically the upper phase rich in FAME, was initially subjected to a qualitative analysis using FTIR to confirm the presence of fatty acid methyl esters in the final product. The region facilitating chemical discrimination between FAME and oils is situated in the 1500–1000  $\text{cm}^{-1}$  range, as emphasized in prior studies [18,21]. According to Torres et al. [18], two distinctive doublets are observable in the 1222–1148  $\text{cm}^{-1}$  and 1475–1419  $\text{cm}^{-1}$  ranges in the FAME spectra, which are conspicuously absent in the oil spectra. The absence of these doublets indicates that the triglycerides in the oil have not undergone a significant conversion to FAME. These observations align with earlier research by Siatis et al. [22], providing further support that these specific wavenumber regions serve as the primary distinguishing features between FAME and oil spectra. To qualitatively assess the presence of doublets in biofuel samples, FTIR spectra were obtained, followed by a quantitative analysis of the FAME content using gas chromatography. In cases where the doublets were absent, measurements by chromatography were avoided to prevent potential damage to the column. The analysis of fatty acid methyl esters (FAME) content from biofuels was performed in accordance with the UNE-EN 14103 standard [23]. The analysis was executed using a 3900 Varian gas chromatograph (GC-FID, CP-8410 model, Holland) equipped with an auto-sampler and the data acquisition software Star Workstation 6.0. Additional details about the method are described in the Supplementary Information. The FTIR spectrophotometer (Agilent Cary 630 FTIR, G8043AA model number, USA) was utilized for the qualitative determination of FAME in the reaction products, following the procedure outlined in the oil characterization.

## 3. Results and discussions

### 3.1. Synthesis and characterization of basic heterogeneous catalyst (HCP-SB-K)

The synthesis of the basic hypercrosslinked catalyst (HCP-SB-K) was carried out in two steps (Fig. 2). In the first one, the hypercrosslinked polymer (HCP-SB) was obtained through mechanochemical polymerization of styrene and benzaldehyde using dimethoxymethane as cross-linking agent. The synthesis of HCPs consists of a Friedel–Crafts alkylation of aromatic monomers using external crosslinkers or chlorinated solvents to join the monomers [24,25]. To avoid the use of chlorinated solvents, mechanochemical polymerization has emerged as an alternative to the synthesis of HCPs by convectional solvent strategy that also reduces the time of reaction from 12 to 48 to 1 h [26]. In the second step, HCP-SB was loaded with potassium nitrate by impregnation method and then, the mixture was calcinated at 350 °C for 2 h under  $\text{N}_2$  atmosphere. In these conditions the potassium nitrate was decomposed due to a redox reaction with the reducing groups, the aldehyde and vinyl groups, obtaining  $\text{K}_2\text{O}$  as basic sites [27]. The estimated cost of the developed catalyst encompasses the expense of reagents, amounting to 2.34 euros per gram, and the energy consumption during synthesis,

totaling 0.988 euros. The total cost per gram of catalyst is 3.328 euros. Detailed calculations for both components can be found in the supplementary information (Section VII. Estimated cost of developed catalyst)."

The IR spectroscopy of HCP-SB (Fig. 3a) shows two bands at 1600 and 1690  $\text{cm}^{-1}$  characteristic of vinyl and aldehyde groups which confirmed the incorporation of both monomers within the network. The two bands at 2980 and 2890  $\text{cm}^{-1}$  are attributed to the methylene linkages between the aromatic rings. After impregnation with  $\text{KNO}_3$ , the characteristics band of vinyl and aldehyde groups remain, but emerges a new one, very intense, at 1384  $\text{cm}^{-1}$  characteristic of the vibration peak of N—O of nitrate. After the treatment at 350 °C, this peak disappears while the bands at 2980 and 2890  $\text{cm}^{-1}$  confirm that the methylene linkages between the aromatic rings remain after the thermal treatment. In fact, the  $^{13}\text{C}$  NMR solid spectra of both polymers (Fig. S2 of the Supplementary Information) show the presence of methylene carbons at 40 ppm. The spectrum of HCP-SB-K shows an intense peak at 170 ppm characteristic of carboxylic acid groups which indicates that during the thermal treatment, the aldehyde groups are oxidized to carboxylic acid groups. This behavior was also observed in the work reported by Lu et al. [27]. The intense signal between 120 and 150 ppm can be attributed to the aromatic carbons present in both networks.

The XPS analysis (Fig. 3b) confirmed the presence of  $\text{K}_2\text{O}$  basic sites due to the appearance of two peaks with energy binding energies of 296.30 and 299.25 eV assigned to  $\text{K}^+$  and  $\text{K}-\text{O}$  species respectively [28], besides a broad peak at 287.68 ascribed to oxidized carbons [27].

The thermal stability of HCP-SB and HCP-SB-K was examined by thermogravimetric analysis (Fig. 3c). As it can be observed both networks showed excellent thermal stability with degradation temperatures of 370 and 350 °C. The unexpectedly high residue observed in HCP-SB network was attributed to residual  $\text{FeCl}_3$  that remains in the network despite its extensive washing. The oxidation of the residual  $\text{FeCl}_3$  during the thermogravimetric analysis generates the appearance of a  $\text{Fe}_2\text{O}_3$  residue, which was used to estimate the amount of Fe in the network, which turned out to be 20%. It is assumed that this content of iron is present also in the HCP-SB-K catalyst.

The  $\text{N}_2$  adsorption/desorption isotherms (Fig. 3d) revealed a mesoporous character both for, the initial HCP and for the network with basic character, HCP-SB-K but the specific surface area decreased from 158 to 28  $\text{m}^2/\text{g}$  probably due to partial damage to the polymeric structure during heat treatment. This behavior has been previously observed in heat treatments and calcination of other HCPs [27]. The pore size revealed that the maximum volume adsorption was achieved in pores of 5 nm size (the pore size distribution of HCP-SB-K is shown in Fig. S3 of the Supplementary Information). It is beneficial because the average pore diameter is comparable to the size of the triglyceride molecule (5 nm); this suggests that triglyceride molecules can easily move through the catalyst's pores, ensuring effective contact between the reactants and the catalyst's surface. This contact is necessary for the transesterification reaction to happen [29]. The morphology of HCP-SB-K was examined by SEM (Fig. 3f). As it can be observed, despite the moderate surface area, the catalyst shows the typical morphology of a

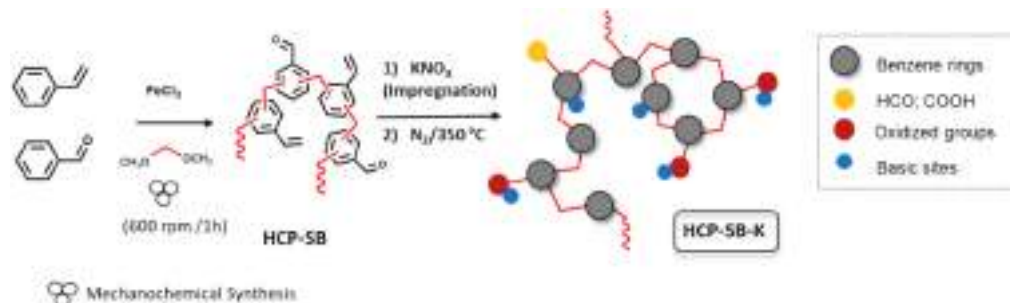


Fig. 2. Scheme of synthesis of the basic hypercrosslinked polymer HCP-SB-K.

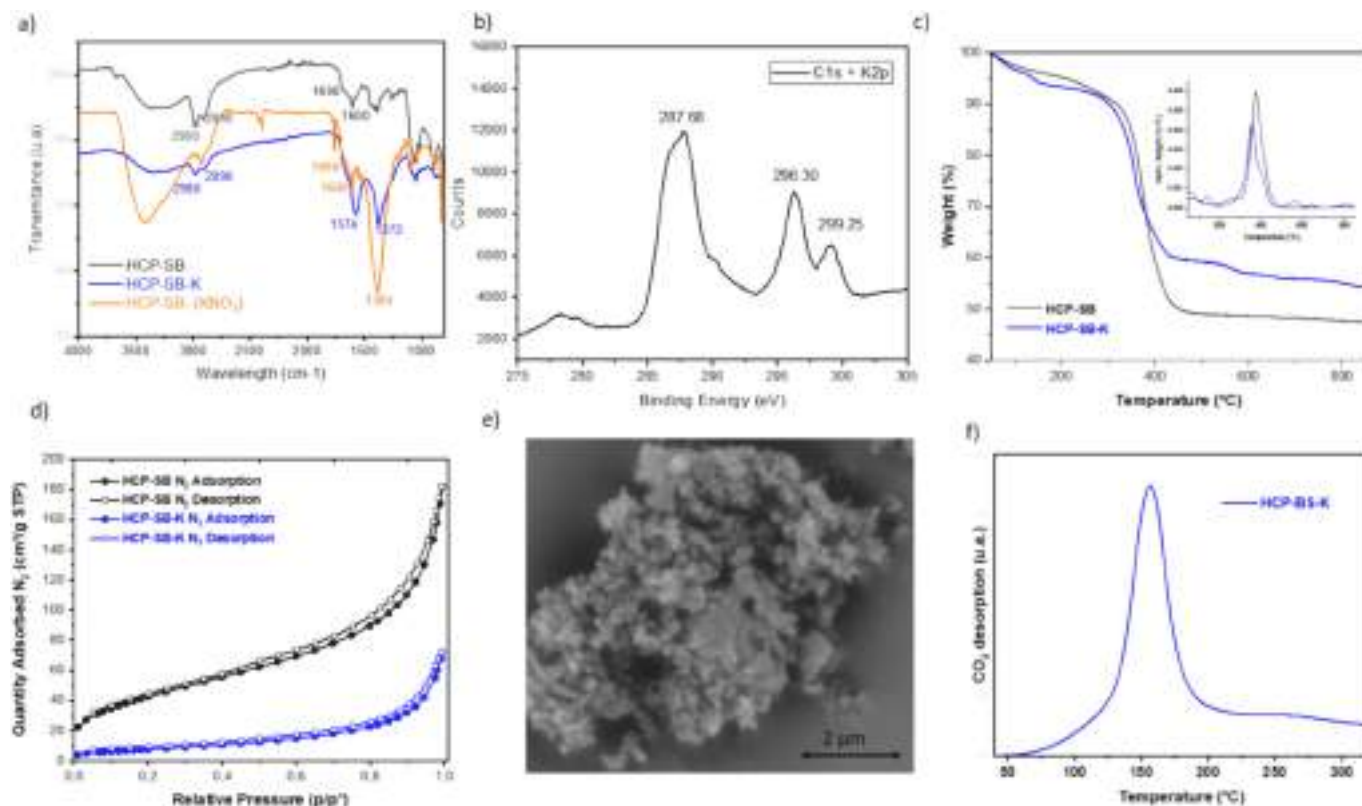


Fig. 3. a) FT-IR spectra, b) XPS spectrum for C1s-K2p, c) TGA and DTGA, d) N<sub>2</sub> adsorption/desorption isotherms, e) SEM images and f) CO<sub>2</sub>-TPD profile of HCP-SB-K.

porous polymer formed by spherical aggregates.

To assess the strength of basic sites, HCP-SB-K was characterized by temperature-programmed desorption of CO<sub>2</sub> (CO<sub>2</sub>-TPD) (Fig. 3e). The maximum temperature obtained of 156 °C corresponds to the desorption of CO<sub>2</sub>, adsorbing an amount of 2.35 mmol/g per gram of catalytic material. This finding signifies the ability of the material to adsorb CO<sub>2</sub>, which is indicative of the presence of basic sites within the material. The strength of these basic sites can be correlated with the observed desorption temperature, with higher desorption temperatures typically associated with stronger basicity. In this context, the desorption temperature of 156 °C suggests the presence of relatively weak basic sites [30]. This observation highlights the potential of the material for use in applications involving base-catalyzed reactions within catalysis, where such weak basic sites may play a specific and valuable role.

### 3.2. Characterization of oils

Table 1 presents the key properties of the feedstocks used in the study for the transesterification reaction. Furthermore, from a comparative point of view, the limits of the parameters established by regulations for biodiesel were included [31].

The acid value of oils is a critical parameter directly linked to their free fatty acid (FFA) content. Lower acid values, as observed in

sunflower oil with an acid value of 0.44 mg<sub>KOH</sub> g<sup>-1</sup>, signify a reduced presence of FFA, making it an attractive choice for biodiesel production. Conversely, oils like *Jatropha curcas*, with a higher acid value of 5.83 mg<sub>KOH</sub> g<sup>-1</sup>, indicate a more substantial FFA content. Understanding acid values is pivotal since elevated FFA levels can impede the transesterification process, leading to reduced biodiesel yields and potentially necessitating additional purification steps. It is important to highlight that the acid value of biodiesel should not exceed 0.5 mg<sub>KOH</sub> g<sub>oil</sub><sup>-1</sup>; it is noteworthy that all oils, except for sunflower oil, surpass this specified threshold (Table 1).

Viscosity is another crucial property of oils and has a direct impact on the flow and handling of the feedstock in biodiesel production. Oils with lower viscosities, such as *Jatropha curcas* esterified oil (16.29 mm<sup>2</sup> s<sup>-1</sup>), exhibit improved flow characteristics and are easier to process during transesterification. In contrast, oils with higher viscosities like Waste Cooking oils (30.06–33.55 mm<sup>2</sup> s<sup>-1</sup>) may require additional heating or agitation to facilitate the reaction process effectively. For a biofuel to be considered biodiesel, the viscosity parameter must be between 3.5 and 5.0 mm<sup>2</sup> s<sup>-1</sup> at 40 °C. Thus, understanding viscosity is vital for optimizing process conditions in biodiesel production.

The density of oils plays a role in determining the volume of oil required for biodiesel production. Lower-density oils offer advantages in terms of ease of handling and transport due to reduced weight per unit volume. On the other hand, oils with higher densities, like Waste Cooking II (0.926 g cm<sup>-3</sup>), may necessitate special considerations during transportation and storage. Despite this, it is important to highlight that the density of biodiesel should fall within the range of 0.860–0.900 g cm<sup>-3</sup> at 15 °C, which is lower than the density values of oils.

The FTIR spectra of oils used as feedstock for biodiesel production are depicted in Fig. 3a. These spectra exhibit a similar shape, regardless of their respective origins. This similarity is primarily due to the presence of common functional groups and chemical bonds in all types of oils. Notably, peaks associated with C=O (carbonyl group) stretching vibrations within the 1735–1750 cm<sup>-1</sup> range are observed (Fig. 4a). This

Table 1

Properties of oils used as feedstock for biodiesel production.

Oil	AV (mg <sub>KOH</sub> g <sub>oil</sub> <sup>-1</sup> )	U <sub>40°C</sub> (mm <sup>2</sup> s <sup>-1</sup> )	ρ <sub>15°C</sub> (g cm <sup>-3</sup> )
Sunflower	0.44	27.23	0.918
<i>Jatropha curcas</i> esterified	1.11	16.29	0.914
Waste Cooking I	2.00	30.10	0.925
Waste Cooking II	3.36	30.06	0.926
Waste Cooking III	4.48	33.55	0.921
<i>Jatropha curcas</i>	5.83	22.65	0.914
Biodiesel	0.5 máx.	3.5–5.0	0.860–0.900

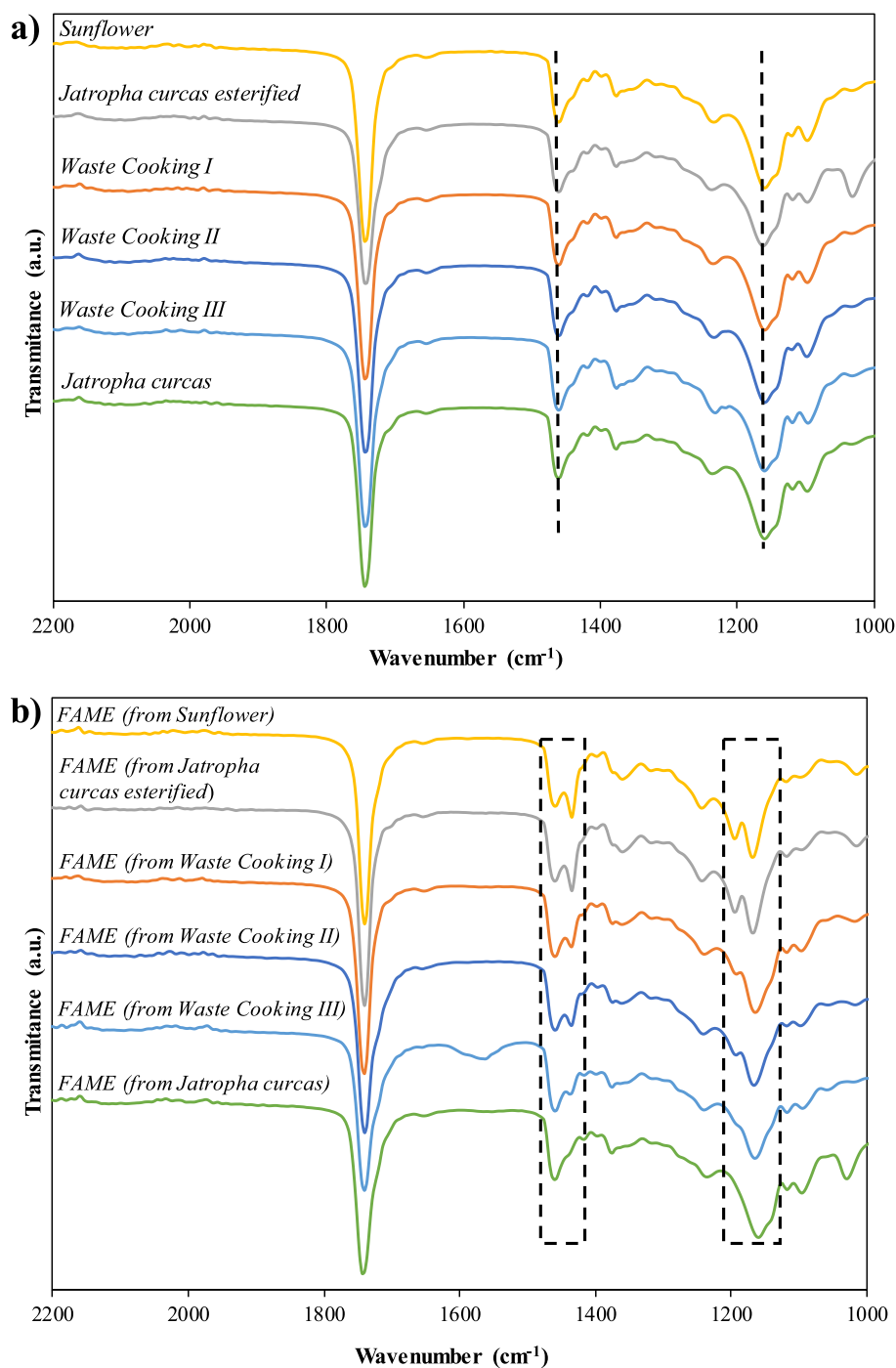


Fig. 4. FTIR spectra of a) oil samples and b) FAME from oil samples.

functional group is a common constituent present in various oil components, including triglycerides and fatty acids.

### 3.3. Catalytic activity

First, the influence of reaction time using sunflower oil was investigated within a range of 0.5 to 2 h (Table 2, entries 1–3). Fig. 5 shows the influence of the reaction time on the FAME content of the reaction product. It was observed that as the reaction time increased while keeping all other conditions constant, the FAME content in the main reaction product also increased. Specifically, at 0.5 h, it reached 63.6% (Table 2, entry 1), at 1 h, it surged to 92.13% (Table 2, entry 2), and at 2 h, it nearly reached completion at 99.9% (Table 2, entry 3). This

demonstrates the high catalytic activity of the HCP-SB-K catalyst in the transesterification reaction for biodiesel production. The remarkable ability of the catalyst to achieve a FAME content of 92.1% within just one hour underscores its efficiency and effectiveness in facilitating the conversion of feedstock into biodiesel. This heightened catalytic activity can be attributed to the interplay of two key factors. Firstly, the average pore diameter closely aligns with the dimensions of triglyceride molecules (5 nm), implying that triglyceride molecules can readily traverse the catalyst's pores, ensuring efficient contact between reactants and the catalyst's surface. Secondly, the catalyst's surface features an abundant presence of basic sites, which significantly contributes to its enhanced performance, particularly when sunflower oil is employed as feedstock.

The mechanism proposed for the transesterification of triglycerides

**Table 2**  
FAME content from transesterification reactions using several feedstock<sup>a)</sup>.

Entry	Oil	AV (mg <sub>KOH</sub> g <sub>oil</sub> <sup>-1</sup> )	Time (h)	Catalyst	FAME (%)
1	Sunflower	0.44	0.5	HCP-SB-K	63.6 ± 1.4
2			1	HCP-SB-K	92.1 ± 0.7
3			2	HCP-SB-K	99.9 ± 0.2
4			2 <sup>b)</sup>	none	63.2 ± 1.4
5			2	HCP-SB	–
6			2	FeCl <sub>3</sub> <sup>c)</sup>	–
7			2	Used HCP-SB-K	42.5 ± 1.6
8			2	Regenerated HCP-SB-K	98.2 ± 0.5
9	<i>Jatropha curcas</i> esterified	1.11	1		75.9 ± 1.2
10	Waste Cooking I	2.00	1		36.1 ± 1.5
11	Waste Cooking II	3.36	1		21.9 ± 1.7
12	Waste Cooking III	4.48	1		11.4 ± 1.4
13	<i>Jatropha curcas</i>	5.83	1		–

a) Condition reactions: oil (1 g), catalyst (30 mg), methanol (7.29 g), 60 °C; b) After 0.5 h, the catalyst was removed for leaching evaluation; c) 6 mg.

using the HCP-SB-K catalyst is depicted in Fig. 6. The transesterification reaction involves three main steps: adsorption of methanol on the basic sites, nucleophilic attack on the triglyceride molecule, and desorption of reaction products. In the first step, methanol is adsorbed onto the basic sites of the HCP-SB-K catalyst, leading to the formation of methoxide ion (CH<sub>3</sub>O<sup>-</sup>). This adsorption process facilitates the removal of a proton from methanol, resulting in the generation of the methoxide anion. Subsequently, in the second step, the methoxide anion attacks the carbonyl carbon of the triglyceride molecule, forming a tetrahedral intermediate. In the final step, the resulting intermediate undergoes rearrangement, leading to the desorption of the -OH group and alkyl triglycerides. This process results in the formation of fatty acid methyl

esters (FAME) and a diglyceride anion. This sequence of events repeats until methoxide ions have attacked all three carbonyl centers of the triglyceride, ultimately yielding three molecules of FAME and one molecule of glycerol. Similar mechanisms for the transesterification reaction using catalysts featuring basic sites have been proposed by various researchers [5,32,33].

Moreover, the influence of FFA content from various oils on the FAME content in the biodiesel product was assessed. All experiments were conducted with a one-hour reaction time. Fig. 7 illustrates the influence of the acidity value of the feedstock on the FAME content of the reaction product. Notably, the highest FAME content was obtained with sunflower oil, which had the lowest FFA content (0.44 mg<sub>KOH</sub> g<sub>oil</sub><sup>-1</sup>), achieving a remarkable 92.1%. However, as the FFA content increased, a decrease in FAME content was observed (Table 2, entries 9–13, and Fig. 7). *Jatropha curcas* esterified oil (1.11 mg<sub>KOH</sub> g<sub>oil</sub><sup>-1</sup>) resulted in 75.9% FAME, while waste cooking I oil (2.00 mg<sub>KOH</sub> g<sub>oil</sub><sup>-1</sup>) yielded 36.1% FAME. Waste cooking II oil (3.36 mg<sub>KOH</sub> g<sub>oil</sub><sup>-1</sup>) produced 21.9% FAME, and waste cooking III oil (4.48 mg<sub>KOH</sub> g<sub>oil</sub><sup>-1</sup>) showed 11.4% FAME. In the case of *Jatropha curcas* (5.83 mg<sub>KOH</sub> g<sub>oil</sub><sup>-1</sup>), the formation of soaps occurred, making it impossible to measure the amount of FAME content. This phenomenon can be attributed to the competitive adsorption of FFA on the active sites of the catalyst. In Fig. 4b, the FTIR spectra of the main product obtained in the transesterification reaction reveal the characteristic doublets corresponding to FAME. Furthermore, it is evident that as the FFA content of the oil increases, these doublets gradually diminish, indicative of a reduced reaction yield. When the FFA levels are elevated, they tend to occupy the catalyst's active sites, reducing the availability of these sites for the transesterification of triglycerides. The presence of a higher concentration of FFA essentially competes with the desired triglycerides for the catalyst's attention, thereby inhibiting the transesterification reaction. Consequently, this competition results in a diminished conversion of triglycerides into fatty acid methyl esters (FAME), leading to a decreased FAME yield and, consequently, a reduction in the catalyst's overall catalytic efficiency. Still, the HCP-SB-K catalyst has exhibited exceptional performance when applied to oils with moderate levels of FFA, demonstrating that the catalyst's basic sites are sufficient for oils with moderate FFA content.

To confirm the essential role of the basic centers in this catalyst, a control experiment was conducted utilizing the initial support, namely HCP-SB, as a catalyst (Table 2, entry 5), with sunflower oil as the feedstock. Notably, no transesterification product was obtained,

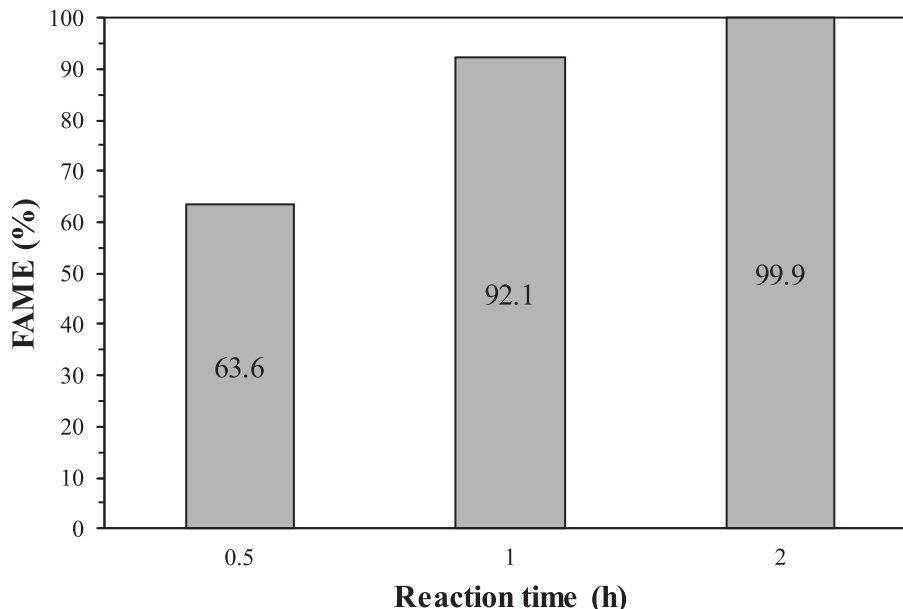


Fig. 5. Influence of the reaction time on the FAME content of the reaction product. Condition reactions: 1 g sunflower oil, 30 mg catalyst, 7.29 g methanol and 60 °C.

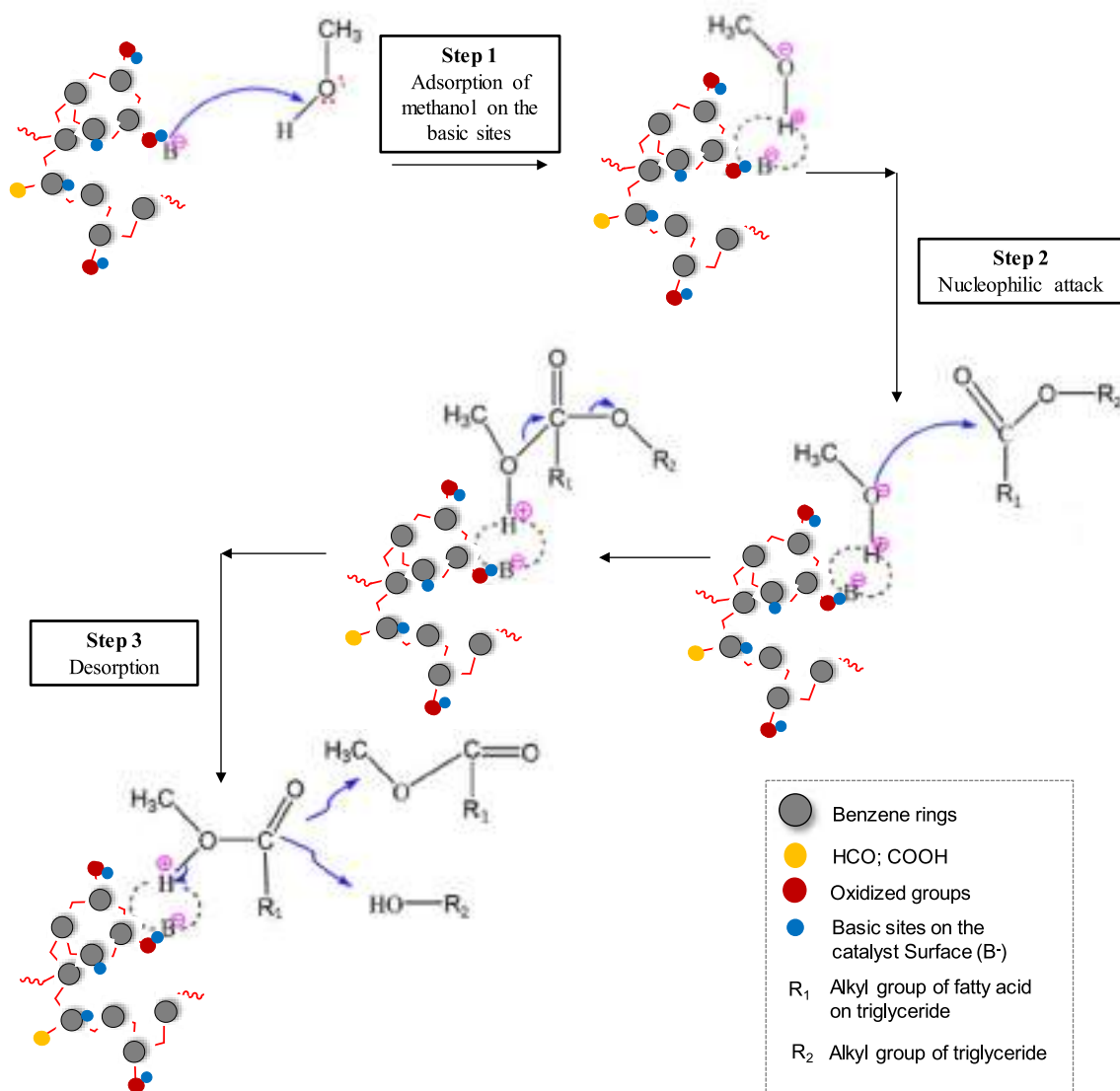


Fig. 6. Mechanism of transesterification reaction with base sites of HCP-SB-K.

signifying the absence of two-phase products in the transesterification reaction, and the absence of characteristic doublets in the FTIR spectrum. This indicates that the triglycerides in the oil did not convert to FAME. HCP-SB demonstrates no catalytic activity for this reaction.

Given that the catalyst contained 20% FeCl<sub>3</sub>, an additional control experiment was conducted using FeCl<sub>3</sub> as a catalyst to assess the influence of this salt on the reaction (Table 2, entry 6). Similarly, no transesterification product was observed under these conditions.

Considering its nature as a hypercrosslinked polymer (HCP), opportunities for further enhancement can be explored. One promising avenue is the modification of the surface active sites, for instance by the introduction of acidic sites. This strategic transformation could render a bifunctional catalyst, allowing it not only to transesterify triglycerides but also to esterify free fatty acids. This dual capability holds the potential to revolutionize biodiesel production. The HCP-SB-K catalyst, armed with its ability to efficiently process oils with moderate FFA content, could become a versatile solution, accommodating a broader range of feedstocks. By addressing both triglycerides and FFA, it opens new horizons for biodiesel production. This adaptability not only simplifies the feedstock requirements but also reduces the need for additional pretreatment steps. Thus, the HCP-SB-K catalyst presents an exciting prospect for more efficient and cost-effective biodiesel

production, marking a significant advancement in sustainable energy solutions.

#### 3.4. Catalyst leaching evaluation

The gradual decline in catalytic activity over time presents a significant and persistent concern in industrial catalytic processes employing heterogeneous catalysts. Deactivation mechanisms stem from both chemical and mechanical factors [34]. Particularly, when utilizing polymer-supported catalysts, it is crucial to prevent the leaching of active components from the solid support. To assess basic site leaching in the HCP-SB-K catalyst, a transesterification reaction with sunflower oil was conducted. After 0.5 h of reaction, the HCP-SB-K catalyst was separated from the reaction mixture, yielding 63.6% (Table 2, entry 1). Subsequently, the reaction mixture, without the catalyst, was continuously stirred for an additional 2 h. Notably, the yield remained virtually unchanged at 63.2% (Table 2, entry 4), indicating the absence of any leaching of basic sites.

#### 3.5. Recycling and regeneration evaluation

Motivated by these findings, tests to assess the recyclability of the

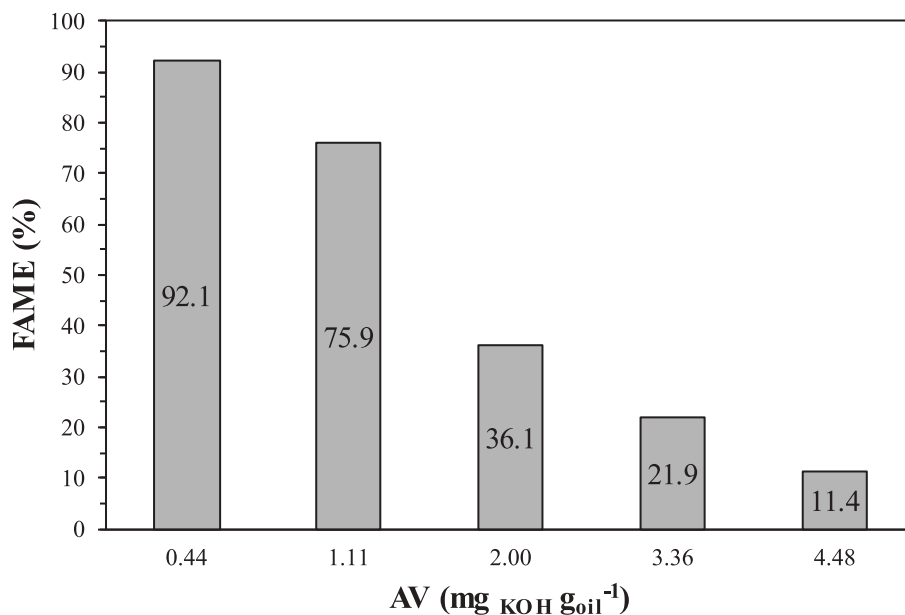


**Fig. 7.** Influence of the acidity value of the feedstock on the FAME content of the reaction product. Condition reactions: 1 g oil, 30 mg catalyst, 7.29 g methanol, 1 h and 60 °C.

HCP-SB-K catalyst was conducted. The transesterification reaction was repeated with the used HCP-SB-K. A reduction in catalytic activity was observed, yielding 99.9% of FAME in the first run and 42.5% in the second run (Table 2, entry 7). Fig. 8 illustrates the change in catalytic activity when HCP-SB-K catalyst was reused. Martín Alonso et al. [35] found a similar behavior when potassium supported on alumina was used as a catalyst. No morphological changes on the surface texture of the catalyst were observed in the SEM images (Fig. 9) after its use in the transesterification reaction, and no differences in the peaks in the FTIR spectra were noted either (Fig. S4 of the Supplementary Information). Nevertheless, a slight decrease in the potassium content of the catalytic material following the transesterification reaction was observed (from 210 mg K/g HCP-SB-K to 170 mg K/g used HCP-SB-K), which is causing the decrease in the transesterification reaction.

Unlike other studies involving acid catalysts, which often include

more recycling studies [36,37], additional cycles were not pursued in this case because the FAME content dropped below the standard requirement of 96.5% [31]. Thus, in order to recover the catalytic activity of the catalyst, its regeneration was carried out. The results show that the regenerated catalyst (Table 2, entry 8), exhibited FAME content very similar to the first run with the fresh catalyst, 98.2% FAME (Fig. 8). This observation strongly supports the notion that the HCP-SB-K catalyst can be regenerated without any noticeable deactivation. This, coupled with the catalyst's straightforward preparation, highlights its potential for industrial applications.

### 3.6. Catalyst performance

To evaluate the catalytic performance of HCP-SB-K as a catalyst in this reaction, a comparative analysis was conducted with other

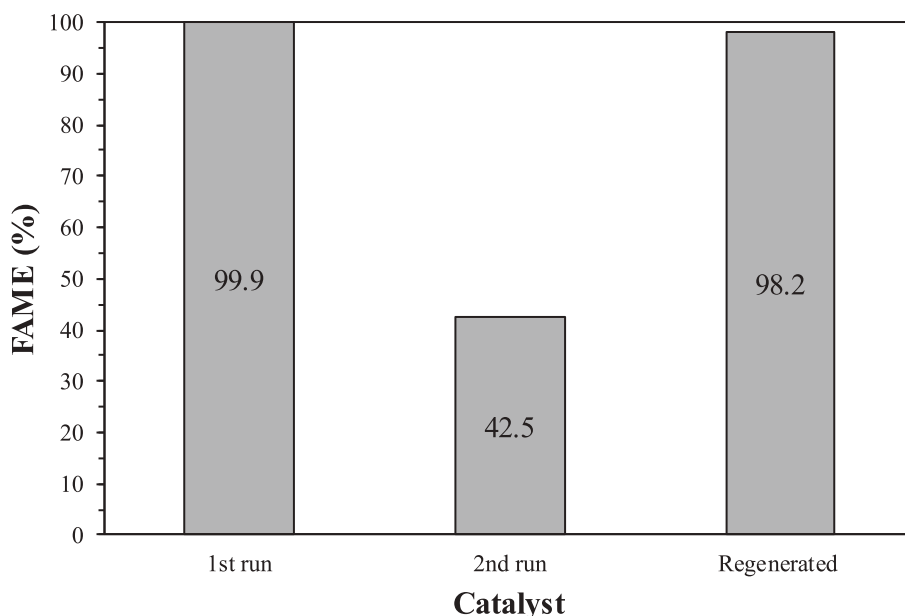


**Fig. 8.** Recycling and regeneration evaluation of HCP-SB-K catalyst in transesterification reaction.

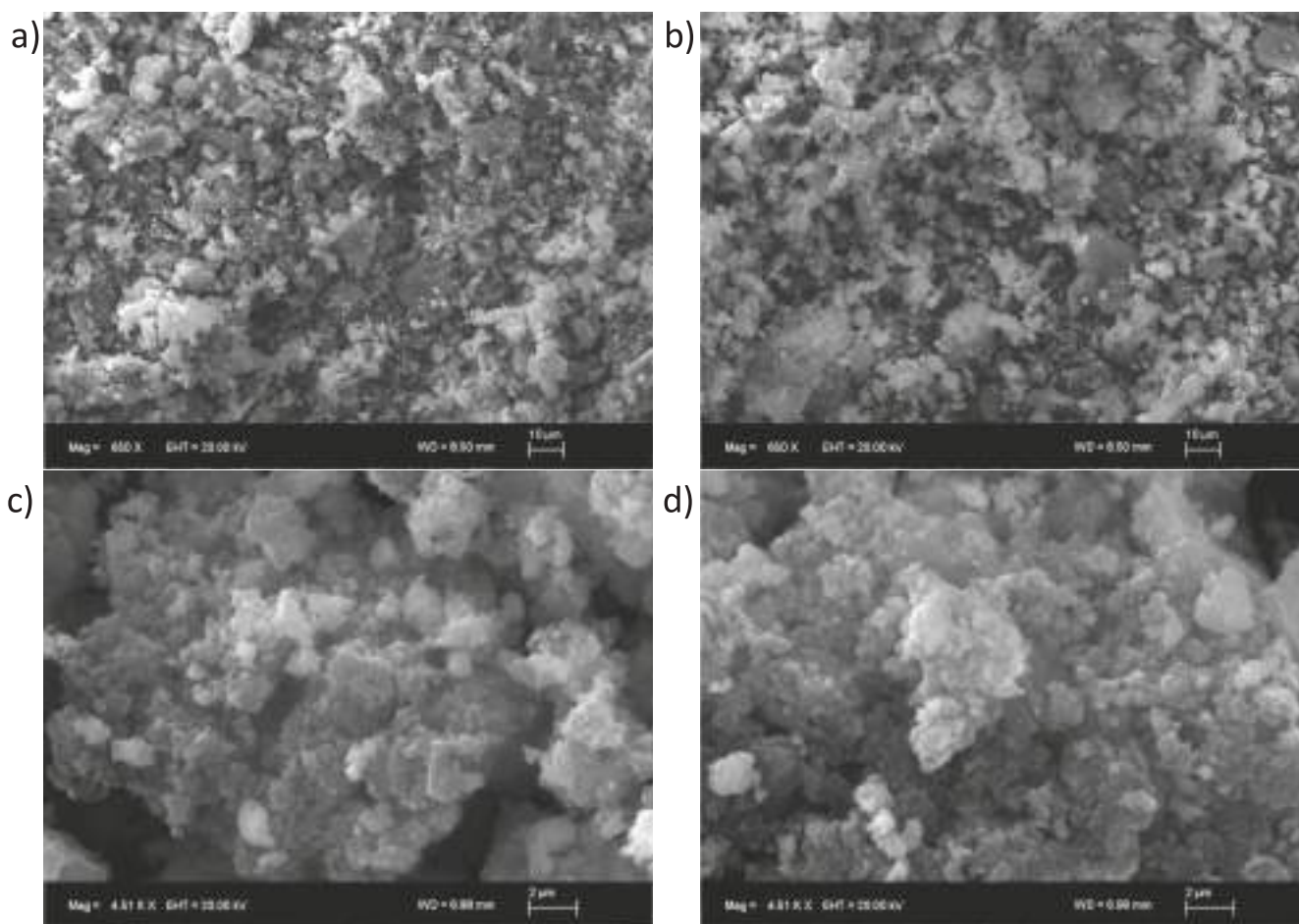


Fig. 9. SEM images of HCP-SB-K with different magnitude a) and c) fresh HCP-SB-K; b) and d) used HCP-SB-K.

homogeneous and heterogeneous basic catalysts documented in the literature for the transesterification reaction, employing similar reaction conditions (Table 3). Generally, when homogeneous catalysts are utilized, FAME contents ranging from 52.8% to 86.9% are achieved. Oils with higher FFA content exhibit lower FAME yields. In the case of low acidity oils, such as sunflower oil, the %FAME obtained with HCP-SB-K surpasses that achieved with the conventional homogeneous basic catalyst (KOH), with the additional advantage of being a solid catalyst. Upon completion of the reaction, there is no need to wash the biodiesel to remove the dissolved catalyst, and no wash water is generated. Comparing the %FAME of HCP-SB-K with the widely employed heterogeneous catalyst (CaO), it is observed that under similar reaction conditions and with low acidity oils, CaO exhibits a lower FAME yield than HCP-SB-K. When CaO is impregnated with K, as shown in Table 3, the %FAME in the biodiesel increases, similar to the trend observed with HCP-SB-K. Extending the reaction time with the HCP-SB-K catalyst, using raw materials with higher FFA content, could potentially enhance the %FAME, extending from 1 to 3 h, as demonstrated by Encinar et al. [38]. Moreover, recent research has utilized CaO derived from solid blast furnace dust waste as a catalyst and oils with relatively high free fatty acid (FFA) content [43]. However, achieving FAME contents of 87.67% necessitates high temperatures (148.95 °C). Conversely, Elouahed et al. [44] and Amal et al. [45] employed CaO-supported bimetallic Molybdenum-Zinc (Mo<sub>7</sub>-Zn<sub>3</sub>) and Fe-CaO catalysts for transesterification of waste cooking oil and chicken oil, respectively. They achieved FAME yields of 95% and 83%, operating under higher temperature and time conditions compared to this study, although with similar catalyst quantities. Thus, the production conditions of biodiesel with catalyst HCP-SB-K are competitive, also being a metal-free catalyst.

#### 4. Conclusions

The synthesis and characterization of the basic hypercrosslinked polymeric catalyst, HCP-SB-K, was carried out featuring a two-step procedure, involving a sustainable mechanochemical polymerization followed by an impregnation with KNO<sub>3</sub> and -calcination process. The FT-IR, <sup>13</sup>C NMR and XPS analyses confirmed the structure of the catalysts and the presence of K<sub>2</sub>O as basic sites. The catalyst exhibited excellent thermal stability and mesoporous characteristics. CO<sub>2</sub>-TPD analysis confirmed the presence of weak basic sites. Employing various feedstocks, the catalytic activity of HCP-SB-K was investigated, revealing its efficiency in transesterification reactions, achieving remarkable FAME content within short reaction times. The influence of FFA content on FAME yield was explored, demonstrating the catalyst's effectiveness with oils containing moderate FFA levels. Control experiments with HCP-SB and FeCl<sub>3</sub> underscored the necessity of basic centers for catalytic activity. The catalyst's recyclability and regeneration capability were demonstrated, further highlighting its potential for industrial applications. Comparative analyses with other catalysts showcased the superior performance of HCP-SB-K, particularly with low-acidity oils, emphasizing its advantages as a metal-free solid, easily recoverable catalyst. The study concludes with a proposal to explore the modification of surface active sites for potential bifunctionality, expanding the catalyst's applicability in biodiesel production and presenting a promising avenue for more efficient and cost-effective processes.

Table 3

Comparison of the activity of different homogeneous and heterogeneous catalysts in the transesterification reaction.

Catalyst	Oil	Reaction conditions	FAME (%)	Ref.	
Homogeneous	KOH	Sunflower (0.2 mg <sub>KOH</sub> g <sub>oil</sub> <sup>-1</sup> ) w/w	55 °C, 2 h, Cat. = 0.5%	86.9 [39]	
	KOH	<i>Jatropha curcas</i> (1.5 mg <sub>KOH</sub> g <sub>oil</sub> <sup>-1</sup> ) w/w	55 °C, 2 h, Cat. = 0.5%	52.8	
	KOH	Waste Cooking (2.0 mg <sub>KOH</sub> g <sub>oil</sub> <sup>-1</sup> ) w/w	60 °C, 4 h, Cat. = 0.5%	70.2	
Heterogeneous	CaO	Sunflower	75 °C, 45 min, Cat. = 1.2% w/w	80 [40]	
	CaO	Soybean (0.2 mg <sub>KOH</sub> g <sub>oil</sub> <sup>-1</sup> ) w	62 °C, 1 h, Cat. = 6% w/w	85 [41]	
	KOH/CaO	<i>Jatropha curcas esterified</i> w	70 °C, 3 h, Cat. = 6% w/w	96.1 [42]	
	KNO <sub>3</sub> /CaO	Rape (2.3 mg <sub>KOH</sub> g <sub>oil</sub> <sup>-1</sup> ) w	65 °C, 3 h, Cat. = 1% w/w	98 [38]	
	CaO from blast furnace waste	Palm + oleic acid (8.9 mg <sub>KOH</sub> g <sub>oil</sub> <sup>-1</sup> ) w/w	148.95 °C, 2 h, Cat. = 7.96% w/w	87.67 [43]	
	MO <sub>7</sub> -Zn <sub>3</sub> /CaO	Waste cooking (3.5 mg <sub>KOH</sub> g <sub>oil</sub> <sup>-1</sup> ) w/w	62.7 °C, 2.27 h, Cat. = 3.37% w/w	95 [44]	
	Fe-CaO	Chicken oil (1.30 mg <sub>KOH</sub> g <sub>oil</sub> <sup>-1</sup> ) w	65 °C, 5 h, Cat. = 3% w/w	83 [45]	
	HCP-SB-K	Sunflower (0.44 mg <sub>KOH</sub> g <sub>oil</sub> <sup>-1</sup> ) w/w	60 °C, 2 h, Cat. = 3.0%	99.9	This work
		Sunflower (0.44 mg <sub>KOH</sub> g <sub>oil</sub> <sup>-1</sup> ) w/w	60 °C, 1 h, Cat. = 3.0%	92.1	
		<i>Jatropha curcas</i> (1.11 mg <sub>KOH</sub> g <sub>oil</sub> <sup>-1</sup> ) w/w	60 °C, 1 h, Cat. = 3.0%	75.9	

### CRedit authorship contribution statement

**S. Señorans:** Writing – original draft, Methodology, Investigation, Formal analysis. **E. Rangel-Rangel:** Writing – original draft, Methodology, Investigation, Formal analysis. **E.M. Maya:** Writing – review & editing, Writing – original draft, Supervision, Methodology, Investigation, Funding acquisition, Formal analysis, Conceptualization. **L. Díaz:** Writing – review & editing, Writing – original draft, Supervision, Methodology, Investigation, Funding acquisition, Formal analysis, Conceptualization.

### Declaration of Competing Interest

The authors declare that they have no known competing financial interests or personal relationships that could have appeared to influence the work reported in this paper.

### Data availability

Data will be made available on request.

### Acknowledgements

This work was supported by the project CATCO2NVERS funded by the European Union's Horizon 2020 research and innovation program under grant agreement No 101000580. Moreover, the authors express their gratitude to the Ministry of Universities for the provided funding.

### Appendix A. Supplementary data

Supplementary data to this article can be found online at <https://doi.org/10.1016/j.reactfunctpolym.2024.105964>.

### References

- [1] V. Gupta, K.P. Singh, The impact of heterogeneous catalyst on biodiesel production: a review, *Mater. Today: Proc.* 78 (3) (2023) 364–371, <https://doi.org/10.1016/j.matpr.2022.10.175>.
- [2] K.G. Georgogianni, A.K. Katsoulidis, P.J. Pomonis, G. Manos, M.G. Kontominas, Transesterification of rapeseed oil for the production of biodiesel using homogeneous and heterogeneous catalysis, *Fuel Process. Technol.* 90 (2009) 1016–1022, <https://doi.org/10.1016/j.fuproc.2009.03.002>.
- [3] D.T. Oyekunle, M. Barasa, E.A. Gendy, S.K. Tiong, Heterogeneous catalytic transesterification for biodiesel production: feedstock properties, catalysts and process parameters, *Process. Saf. Environ. Prot.* 177 (2023) 844–867, <https://doi.org/10.1016/j.psep.2023.07.064>.
- [4] H. Pan, H. Li, H. Zhang, A. Wang, S. Yang, Functional nanomaterials-catalyzed production of biodiesel, *Curr. Nanosci.* 16 (2020) 376–391, <https://doi.org/10.2174/1573413715666190411142820>.
- [5] S.F. Basumatary, S. Brahma, M. Hoque, B.K. Das, M. Selvaraj, S. Brahma, S. Basumatary, Advances in CaO-based catalysts for sustainable biodiesel synthesis, *Green Energy Resour.* 1 (3) (2023) 100032, <https://doi.org/10.1016/j.gerr.2023.100032>.
- [6] O. Awogbemi, D. Vandi Von Kallon, V.S. Aigbodion, Trends in the development and utilization of agricultural wastes as heterogeneous catalyst for biodiesel production, *J. Energy Inst.* 98 (2021) 244–258, <https://doi.org/10.1016/j.joei.2021.06.017>.
- [7] J.V.L. Ruatpuia, G. Halder, S. Mohan, B. Gurunathan, H. Li, F. Chai, S. Basumatary, S.L. Rokhum, Microwave-assisted biodiesel production using ZIF-8 MOF-derived nanocatalyst: a process optimization, kinetics, thermodynamics and life cycle cost analysis, *Energy Convers. Manag.* 292 (2023) 117418, <https://doi.org/10.1016/j.enconman.2023.117418>.
- [8] S.F. Basumatary, K. Patir, B. Das, P. Saikia, S. Brahma, B. Basumatary, B. Nath, B. Basumatary, S. Basumatary, Production of renewable biodiesel using metal organic frameworks based materials as efficient heterogeneous catalysts, *J. Clean. Prod.* 358 (2022) 131955, <https://doi.org/10.1016/j.jclepro.2022.131955>.
- [9] N. Enjamuri, S. Sarkar, B.M.M. Reddy, J. Mondal, Design and catalytic application of functional porous organic polymers: opportunities and challenges, *Chem. Rec.* 19 (2019) 1782–1792, <https://doi.org/10.1002/tcr.201800080>.
- [10] L. Pan, Q. Chen, J. Zhu, J. Yu, Y. He, B. Han, Hypercrosslinked porous polycarbazoles via one-step oxidative coupling reaction and Friedel–Crafts alkylation, *Polym. Chem.* 6 (2015) 2478, <https://doi.org/10.1039/C4PY01797H>.
- [11] Z. Duana, Y. Wang, Q. Pana, Y. Xieb, Z. Chena, Hypercrosslinking polymers fabricated from Divinyl benzene via Friedel–crafts addition polymerization, *Chin. J. Polym. Sci.* 40 (2022) 310–320, <https://doi.org/10.1007/s10118-022-2667-7>.
- [12] D. Costenaro, F. Carniato, G. Gatti, C. Bisio, L. Marchese, Optimization of the Friedel–crafts alkylation for the synthesis of hyper-cross-linked polymers, *J. Phys. Chem. C* 115 (2011) 25257–25265, <https://doi.org/10.1021/acsapm.2c00973>.
- [13] S. Bhunia, B. Banerjee, A. Bhaumik, A new hypercrosslinked supermicroporous polymer, with scope for sulfonation, and its catalytic potential for the efficient synthesis of biodiesel at room temperature, *Chem. Commun.* 51 (2015) 5020–5023, <https://doi.org/10.1039/c4cc09872b>.
- [14] A. Varyambath, M.R. Kim, I. Kim, Sulfonic acid-functionalized organic knitted porous polyaromatic microspheres as heterogeneous catalysts for biodiesel production, *New J. Chem.* 42 (15) (2018) 12745–12753, <https://doi.org/10.1039/c8nj02720j>.
- [15] K. Srikumar, Y.H. Tan, J. Kandedo, I.S. Tan, N.M. Mubarak, M.L. Ibrahim, N. Y. Peter, H.C.Y. Yek, R.R. Foo, M. Khalid Karri, A review on the environmental life cycle assessment of biodiesel production: selection of catalyst and oil feedstock, *Biomass Bioenergy* 185 (2024) 107239, <https://doi.org/10.1016/j.biombioe.2024.107239>.
- [16] S. Brahma, B. Basumatary, S.F. Basumatary, B. Das, S. Brahma, S.L. Rokhum, S. Basumatary, Biodiesel production from quinary oil mixture using highly efficient *Musa chinensis* based heterogeneous catalyst, *Fuel* 336 (2023) 127150, <https://doi.org/10.1016/j.fuel.2022.127150>.
- [17] S. Brahma, B. Nath, B. Basumatary, B. Das, P. Saikia, K. Patir, S. Basumatary, Biodiesel production from mixed oils: a sustainable approach towards industrial biofuel production, *Chem. Eng. J. Adv.* 10 (2022) 100284, <https://doi.org/10.1016/j.cej.2022.100284>.
- [18] A. Torres, B. Fuentes, K.E. Rodríguez, A. Brito, L. Díaz, Analysis of the content of fatty acid methyl esters in biodiesel by Fourier-transform infrared spectroscopy: method and comparison with gas chromatography, *J. Am. Oil Chem. Soc.* 97 (2020) 651–661, <https://doi.org/10.1002/aocs.12350>.

- [19] UNE-EN 14104, Fat and Oil Derivatives - Fatty Acid Methyl Ester (FAME) - Determination of Acid Value, Comité Europeen de Normalisation (CEN), Madrid, Spain, 2021.
- [20] D.T. Oyekunle, M. Barasa, E.A. Gendy, S. Kiong Tiong, Heterogeneous catalytic transesterification for biodiesel production: feedstock properties, catalysts and process parameters, *Process Saf. Environ. Prot.* 177 (2023) 844–867, <https://doi.org/10.1016/j.psep.2023.07.064>.
- [21] S.N. Rabel, V.P. Ferraz, L.S. Oliveira, A.S. Franca, FTIR analysis for quantification of fatty acid methyl esters in biodiesel produced by microwave-assisted transesterification, *Int. J. Environ. Sci. Dev.* 6 (2015) 964–969, <https://doi.org/10.7763/IJESD.2015.V6.730>.
- [22] N.G. Siatis, A.C. Kimbaris, C.S. Pappas, P.A. Tarantilis, M.G. Polissiou, Improvement of biodiesel production based on the application of ultrasound: monitoring of the procedure by FTIR spectroscopy, *J. Am. Oil Chem. Soc.* 83 (2006) 53–57, <https://doi.org/10.1007/s11746-006-1175-1>.
- [23] UNE-EN 14103, Fat and Oil Derivatives—Fatty Acid Methyl Esters (FAME)—Determination of Ester and Linolenic Acid Methyl Ester Contents, Comité Europeen de Normalisation (CEN), Madrid, Spain, 2020.
- [24] B. Li, R. Gong, W. Wang, X. Huang, W. Zhang, H. Li, C. Hu, B. Tan, A new strategy to microporous polymers: knitting rigid aromatic building blocks by external cross-linker, *Macromolecules* 44 (6) (2011) 2410–2414, <https://doi.org/10.1021/ma200630s>.
- [25] K.J. Msayib, N.B. McKeown, Inexpensive polyphenylene network polymers with enhanced microporosity, *J. Mater. Chem. A* 4 (2016) 10110–10113, <https://doi.org/10.1039/c6ta03257e>.
- [26] S. Grätz, S. Zink, H. Krafczyk, M. Rose, L. Borchardt, Mechanochemical synthesis of hyper-crosslinked polymers: influences on their pore structure and adsorption behaviour for organic vapors, *Beilstein J. Org. Chem.* 15 (2019) 1154–1161, <https://doi.org/10.3762/bjoc.1>.
- [27] X. Lu, S. Shi, G. Zhu, L. Zhao, M. Wang, J. Gao, Z. Du, J. Xu, Generation of strong basic site on Hypercrosslinked porous polymers as catalyst for the catalytic oxidation of methylene compounds, *ChemSelect* 5 (2020) 549–553, <https://doi.org/10.1002/slct.201904370>.
- [28] Z. Zhang, M. Hu, B. Lv, J. Kang, J. Tang, Z. Fei, X. Chen, Q. Liu, M. Cui, X. Qiao, Solvent-assisted stepwise redox approach to generate zeolite NaA-supported K2O as strong base catalyst for Michael addition of ethyl acrylate with ethanol, *ACS Omega* 3 (8) (2018) 10188–10197, <https://doi.org/10.1021/acsomega.8b00704>.
- [29] S.L.C. Ferreira, R.E. Bruns, H.S. Ferreira, G.D. Matos, J.M. David, G.C. Brandao, E. G.P.D. Silva, L.A. Portugal, P.S.D. Reis, A.S. Souza, W.N.L.D.S. Santos, Box-Behnken design: an alternative for the optimization of analytical methods, *Anal. Chim. Acta* 597 (2007) 179, <https://doi.org/10.1016/j.aca.2007.07.011>.
- [30] M. Bolognini, F. Cavani, D. Scagliarini, C. Flego, C. Perego, M. Saba, Heterogeneous basic catalysts as alternatives to homogeneous catalysts: reactivity of mg/Al mixed oxides in the alkylation of m-cresol with methanol, *Catal. Today* 75 (2002) 103–111, [https://doi.org/10.1016/S0920-5861\(02\)00050-0](https://doi.org/10.1016/S0920-5861(02)00050-0).
- [31] UNE-EN 14214, Liquid Petroleum Products - Fatty Acid Methyl Esters (FAME) for use in Diesel Engines and Heating Applications - Requirements and Test Methods, Comité Europeen de Normalisation (CEN), Madrid, Spain, 2013.
- [32] S. Hu, Y. Wang, H. Han, Utilization of waste freshwater mussel shell as an economic catalyst for biodiesel production, *Biomass Bioenergy* 35 (8) (2011) 3627–3635, <https://doi.org/10.1016/j.biombioe.2011.05.009>.
- [33] M. Ahmed, K.A. Ahmad, D.N. Vo, M. Yusuf, A. Haq, A. Abdullah, M. Aslam, D. S. Patle, Z. Ahmad, E. Ahmad, M. Athar, Recent trends in sustainable biodiesel production using heterogeneous nanocatalysts: function of supports, promoters, synthesis techniques, reaction mechanism, and kinetics and thermodynamic studies, *Energy Convers. Manag.* 280 (2023) 116821, <https://doi.org/10.1016/j.enconman.2023.116821>.
- [34] R.M.N. Kalla, M.R. Kim, I. Kim, Sulfonic acid-functionalized, hyper-cross-linked porous polyphenols as recyclable solid acid catalysts for esterification and transesterification reactions, *Ind. Eng. Chem. Res.* 57 (34) (2018) 11583–11591, <https://doi.org/10.1021/acs.iecr.8b02418>.
- [35] D. Martín Alonso, R. Mariscal, R. Moreno-Tost, M.D. Zafra Poves, M. López Granados, Potassium leaching during triglyceride transesterification using K/γ-Al<sub>2</sub>O<sub>3</sub> catalysts, *Catal. Commun.* 8 (2007) 2074–2208, <https://doi.org/10.1016/j.catcom.2007.04.003>.
- [36] N. Ghosh, D. Rhithuparna, R. Khatoun, S.L. Rokhum, G. Halder, Evaluating the scale-up potential of biogenic heterogeneous catalyst for biodiesel production, *ACS Sustain. Resour. Manage.* 1 (3) (2024) 480–492, <https://doi.org/10.1021/acssusresmgmt.3c00111>.
- [37] N. Ghosh, D. Rhithuparna, R. Khatoun, S.L. Rokhum, G. Halder, Sulphonic-acid functionalized novel Limonia acidissima carbonaceous catalyst for biodiesel synthesis from Millettia pinnata oil: optimization, kinetics, thermodynamics and cost analysis, *J. Clean Prod.* 394 (2023) 136362, <https://doi.org/10.1016/j.jclepro.2023.136362>.
- [38] J.M. Encinar, J.F. González, A. Pardal, G. Martínez, Rape oil transesterification over heterogeneous catalysts, *Fuel Process. Technol.* 91 (2010) 1530–1536, <https://doi.org/10.1016/j.fuproc.2010.05.034>.
- [39] L. Díaz Rodríguez, *Procesos de catálisis heterogénea para la obtención de biodiésel. Utilización de aceite de jatropha curcas y aceite de fritura como materias primas*, Universidad de La Laguna, 2018.
- [40] M. Verziu, S.M. Coman, R. Richards, V.I. Parvulescu, Transesterification of vegetable oils over CaO catalysts, *Catal. Today* 167 (2011) 64–70, <https://doi.org/10.1016/j.cattod.2010.12.031>.
- [41] H.A. Choudhury, S. Chakma, V.S. Moholkar, Mechanistic insight into sonochemical biodiesel synthesis using heterogeneous base catalyst, *Ultrason. Sonochem.* 21 (2014) 169–181, <https://doi.org/10.1016/j.ultsonch.2013.04.010>.
- [42] J. Nisar, R. Razaq, M. Farooq, M. Iqbal, R.A. Khan, M. Sayed, A. Shah, I. Rahman, Enhanced biodiesel production from Jatropha oil using calcined waste animal bones as catalyst, *Renew. Energy* 101 (2017) 111–119, <https://doi.org/10.1016/j.renene.2016.08.048>.
- [43] J. Liu, T. Lin, S. Niu, J. Zhu, Z. Yang, J. Geng, S. Liu, Y. Zheng, B. Liang, X. Sun, H. Zhang, Transesterification of acidic palm oil using solid waste/CaO as a bifunctional catalyst, *Fuel* 362 (2024) 30913, <https://doi.org/10.1016/j.fuel.2024.130913>.
- [44] S.K. Elouahed, N. Asikin-Mijan, G. Alsultan, O. Kaddour, M.R. Yusop, H. Mimoun, S. Samidin, N. Mansir, Y.H. Taufiq-Yap, Optimization of the activity of Mo7-Zn3/CaO catalyst in the transesterification of waste cooking oil into sustainable biodiesel via response surface methodology, *Energy Convers. Manag.* 303 (2024) 118185, <https://doi.org/10.1016/j.enconman.2024.118185>.
- [45] R. Amal, R.A. Nadeem, A. Intisar, H. Rouf, D. Hussain, R. Kousar, An insight into the catalytic properties and process optimization of Fe, Ni doped eggshell derived CaO for a green biodiesel synthesis from waste chicken fat, *Catal. Commun.* 187 (2024) 106848, <https://doi.org/10.1016/j.catcom.2024.106848>.